ELSEVIER
Available online at www.sciencedirect.com
ScienceDirect
Comput. Methods Appl. Mech. Engrg. xxx (2007) xxx–xxx
Computer methods in applied mechanics and engineering
www.elsevier.com/locate/cma

A semi-analytical approach for radiation and scattering problems with circular boundaries

J.T. Chen [a,*], C.T. Chen [a], P.Y. Chen [a], I.L. Chen [b]

[a] Department of Harbor and River Engineering, National Taiwan Ocean University, Keelung, Taiwan
[b] Department of Naval Architecture, National Kaohsiung Marine University, Kaohsiung, Taiwan

Received 15 June 2006; received in revised form 22 January 2007; accepted 13 February 2007

Abstract

In this paper, the radiation and scattering problems with circular boundaries are studied by using the null-field integral equations in conjunction with degenerate kernels and Fourier series to avoid calculating the Cauchy and Hadamard principal values. In implementation, the null-field point can be located on the real boundary owing to the introduction of degenerate kernels for fundamental solution. An adaptive observer system of polar coordinate is considered to fully employ the property of degenerate kernels. For the hypersingular equation, vector decomposition for the radial and tangential gradient is carefully considered. This method can be seen as a semi-analytical approach since errors attribute from the truncation of Fourier series. Neither hypersingularity in Burton and Miller approach nor the CHIEF concepts were required to deal with the problem of irregular frequencies. Four gains, well-posed model, singularity free, boundary-layer effect free and exponential convergence are achieved using the present approach. A fast convergence rate in exponential order than algebraic one in BEM stems from the series expansions. Three examples were demonstrated to see the validity of the present formulation and show the better accuracy than BEM.

Keywords: Null-field integral equation; Degenerate kernel; Fourier series; Helmholtz; Radiation; Scattering

1. Introduction

It is well known that boundary integral equation methods have been used to solve exterior acoustic radiation and scattering problems for many years. The importance of the integral equation in the solution, both theoretical and practical, for certain types of boundary value problems is universally recognized. One of the problems frequently addressed in BIEM/BEM is the problem of irregular frequencies in boundary integral formulations for exterior acoustics and water wave problems. These frequencies do not represent any kind of physical resonance but are due to the numerical method, which has non-unique solutions at characteristic frequencies associated with the eigenfrequency of the interior problem. Burton and Miller approach [1] as well as CHIEF technique have been employed to deal with these problems [2].

Numerical examples for non-uniform radiation and scattering problems by using the dual BEM were provided and the irregular frequencies were easily found [3]. The non-uniqueness of radiation and scattering problems are numerically manifested in a rank deficiency of the influence coefficient matrix in BEM [1]. In order to obtain the unique solution, several integral equation formulations that provide additional constraints to the original system of equations have been proposed. Burton and Miller [1] proposed an integral equation that was valid for all wave numbers by forming a linear combination of the singular integral equation and its normal derivative. However, the calculation for the hypersingular integration is required. To avoid the computation of hypersingularity, an alternative method, Schenck [2] used the CHIEF method, which

* Corresponding author. Tel./fax: +886 2 24622192x6177.
E-mail address: jtchen@mail.ntou.edu.tw (J.T. Chen).

0045-7825/$ - see front matter © 2007 Published by Elsevier B.V.
doi:10.1016/j.cma.2007.02.004

employs the boundary integral equations by collocating the interior point as an auxiliary condition to make up deficient constraint condition. Many researchers [5–7] applied the CHIEF method to deal with the problem of fictitious frequencies. If the chosen point locates on the nodal line of the associated interior eigenproblem, then this method fails. To overcome this difficulty, Wu and Seybert [5,6] employed a CHIEF-block method using the weighted residual formulation for acoustic problems. For water wave problems, Ohmatsu [8] presented a combined integral equation method (CIEM), it was similar to the CHIEF-block method for acoustics proposed by Wu and Seybert. In the CIEM, two additional constraints for one interior point result in an overdetermined system to insure the removal of irregular frequencies. An enhanced CHIEF method was also proposed by Lee and Wu [7]. The main concern of the CHIEF method is how many numbers of interior points are selected and where the positions should be located. Recently, the appearance of irregular frequency in the method of fundamental solutions was theoretically proved and numerically implemented [9]. However, as far as the present authors are aware, only a few papers have been published to date reporting on the efficacy of these methods in radiation and scattering problems involving more than one vibrating body. For example, Dokumaci and Sarigül [10] had discussed the fictitious frequency of radiation problem of two spheres. They used the surface Helmholtz integral equation (SHIE) and the CHIEF method to find the position of fictitious frequency. In our formulation, we are also concerned with the fictitious frequency especially for the multiple cylinders of scatters and radiators. At the same time, we may wonder if there is one approach free of both Burton and Miller approach and CHIEF technique.

For the problems with circular boundaries, the Fourier series expansion method is specially suitable to obtain the analytical solution. The interaction of water waves with arrays of vertical circular cylinders was studied using the dispersion relation by Linton and Evans [11]. If the depth dependence is removed, it becomes two-dimensional Helmholtz problem. For membrane and plate problems, analytical treatment of integral equations for circular and annular domains were proposed in closed-form expressions for the integral in terms of Fourier coefficients by Kitahara [12]. Elsherbeni and Hamid [13] used the method of moments to solve the scattering problem by parallel conducting circular cylinders. They also divided the total scattered field into two components, namely a noninteraction term and a term due to all interactions between the cylinders. Chen et al. [3] employed the dual BEM to solve the exterior acoustic problems with circular boundary. Grote and Kirsch [14] utilized multiple Dirichlet to Neumann (DtN) method to solve multiple scattering problems of cylinders. DtN solution was obtained by combining contributions from multiple outgoing wave fields. Degenerate kernels were given in the book of Kress [15]. The mathematical proof of exponential convergence for Helmholtz problems using the Fourier expansion was derived in [16]. According to the literature review, it is observed that exact solutions for boundary value problems are only limited for simple cases, e.g. a cylinder radiator and scatter, half-plane with a semi-circular canyon, a hole under half-plane, two holes in an infinite plate. Therefore, proposing a systematic approach for solving BVP with circular boundaries of various numbers, positions and radii is our goal in this article.

In this paper, the boundary integral equation method (BIEM) is utilized to solve the exterior radiation and scattering problems with circular boundaries. To fully utilize the geometry of circular boundary, not only Fourier series for boundary densities as previously used by many researchers but also the degenerate kernel for fundamental solutions in the present formulation is incorporated into the null-field integral equation. All the improper boundary integrals are free of calculating the principal values (Cauchy and Hadamard) in place of series sum. In integrating each circular boundary for the null-field equation, the adaptive observer system of polar coordinate is considered to fully employ the property of degenerate kernel. To avoid double integration, point collocation approach is considered. Free of worrying how to choose the collocation points, uniform collocation along the circular boundary yields a well-posed matrix. For the hypersingular equation, vector decomposition for the radial and tangential gradients is carefully considered, especially for the eccentric case. Fictitious frequencies in the multiple scatters and radiators are also examined. Nonuniform radiation and scattering problems are solved for a single circular cylinder. Finally, a five-scatters problem in the full plane was given to demonstrate the validity of the present method. The results are compared with those of analytical solution, BEM, FEM and/or other numerical solutions.

2. Problem statement and integral formulation

2.1. Problem statement

The governing equation of the acoustic problem is the Helmholtz equation

$$(\nabla^2 + k^2)u(x) = 0, \quad x \in D, \tag{1}$$

where ∇_2, k and D are the Laplacian operator, the wave number, and the domain of interest, respectively. Consider the radiation and scattering problems containing N randomly distributed circular holes centered at the position vector $\underset{\sim}{c}_j \, (j = 1, 2, \ldots, N)$ as shown in Fig. 1a and b, respectively.

2.2. Dual boundary integral formulation

Based on the dual boundary integral formulation of the domain point [17], we have

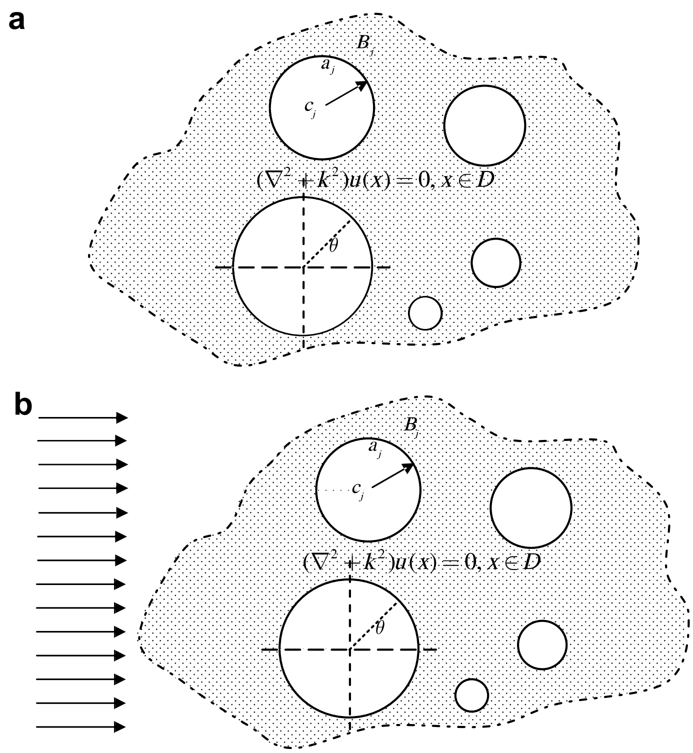

Fig. 1. Problem statement: (a) problem statement for 2-D exterior radiator problem and (b) problem statement for 2-D exterior scattering problem.

$$2\pi u(x)=\int_B T^{\mathrm{i}}(s,x)u(s)\,\mathrm{d}B(s)-\int_B U^{\mathrm{i}}(s,x)t(s)\,\mathrm{d}B(s),\quad x\in D\cup B, \tag{2}$$

$$2\pi t(x)=\int_B M^{\mathrm{i}}(s,x)u(s)\,\mathrm{d}B(s)-\int_B L^{\mathrm{i}}(s,x)t(s)\,\mathrm{d}B(s),\quad x\in D\cup B, \tag{3}$$

where s and x are the source and field points, respectively, B is the boundary. Eqs. (2) and (3) are quite different from the conventional formulation since they are valid not only for the point in the domain D but also for the boundary points if the kernels are properly expressed as the interior (superscript i) degenerate kernels. The set of x in Eqs. (2) and (3) is closed since $x\in D\cup B$. The flux $t(s)$ is the directional derivative of $u(s)$ along the outer normal direction at s. For the interior point, $t(x)$ is artificially defined. For example, $t(x)=\partial u/\partial x_1$, if $\underset{\sim}{n}(x)=(1,0)$ and $t(x)=\partial u/\partial x_2$, if $\underset{\sim}{n}(x)=(0,1)$ where $\widetilde{(x_1,x_2)}$ is the coordinate of field point $\underset{\sim}{x}$. The $U(s,x),T(s,x),L(s,x)$ and $M(s,x)$ represent the four kernel functions [3]

$$U(s,x)=\frac{-\mathrm{i}\pi H_0^{(1)}(kr)}{2}, \tag{4}$$

$$T(s,x)=\frac{\partial U(s,x)}{\partial n_s}=\frac{-\mathrm{i}k\pi H_1^{(1)}(kr)}{2}\frac{y_i n_i}{r}, \tag{5}$$

$$L(s,x)=\frac{\partial U(s,x)}{\partial n_x}=\frac{\mathrm{i}k\pi H_1^{(1)}(kr)}{2}\frac{y_i\bar{n}_i}{r}, \tag{6}$$

$$M(s,x)=\frac{\partial^2 U(s,x)}{\partial n_x\partial n_s}=\frac{-\mathrm{i}k\pi}{2}\left[-k\frac{H_2^{(1)}(kr)}{r^2}y_i y_j n_i\bar{n}_j+\frac{H_1^{(1)}}{r}n_i\bar{n}_i\right], \tag{7}$$

where $H_n^{(1)}(kr)=J_n(kr)+\mathrm{i}Y_n(kr)$ is the nth order Hankel function of the first kind, and J_n is the Bessel function Y_n is the modified Bessel function, $r=|x-s|$, $y_i=s_i-x_i$, $i^2=-1$, n_i and $\bar{n}_i$ are the ith components of the outer normal vectors at s and x, respectively. Eqs. (2) and (3) are referred to singular and hypersingular boundary integral equation (BIE), respectively.

2.3. Null-field integral formulation in conjunction the degenerate kernel and Fourier series

By collocating x outside the domain ($x\in D^{\mathrm{c}}$, complementary domain), we obtain the null-field integral equations as shown below [18]:

$$0=\int_B T^{\mathrm{e}}(s,x)u(s)\,\mathrm{d}B(s)-\int_B U^{\mathrm{e}}(s,x)t(s)\,\mathrm{d}B(s),\quad x\in D^{\mathrm{E}}\cup B, \tag{8}$$

$$0=\int_B M^{\mathrm{e}}(s,x)u(s)\,\mathrm{d}B(s)-\int_B L^{\mathrm{e}}(s,x)t(s)\,\mathrm{d}B(s),\quad x\in D^{\mathrm{E}}\cup B, \tag{9}$$

where the collocation point x can locate on the outside of the domain as well as B if kernels are substituted into proper exterior (superscript e) degenerate kernels. Since degenerate kernels can describe the fundamental solutions in two regions (interior and exterior domain), the BIE for a domain point of Eqs. (2) and (3) and null-field BIE of Eqs. (8) and (9) can include the boundary point. In real implementation, the null-field point can be pushed on the real boundary since we introduce the expression of degenerate kernel for fundamental solutions. By using the polar coordinate, we can express $x=(\rho,\phi)$ and $s=(R,\theta)$. The four kernels, U, T, L and M can be expressed in terms of degenerate kernels as shown below [3]:

$$U(s,x)=\begin{cases} U^{\mathrm{I}}(s,x)=\frac{-\pi i}{2}\sum_{m=0}^{\infty}\varepsilon_m J_m(k\rho)H_m^{(1)}(kR)\cos(m(\theta-\phi)), & R\geqslant\rho,\\ U^{\mathrm{E}}(s,x)=\frac{-\pi i}{2}\sum_{m=0}^{\infty}\varepsilon_m H_m^{(1)}(k\rho)J_m(kR)\cos(m(\theta-\phi)), & \rho>R,\end{cases}\tag{10}$$

$$T(s,x)=\begin{cases} T^{\mathrm{I}}(s,x)=\frac{-\pi k i}{2}\sum_{m=0}^{\infty}\varepsilon_m J_m(k\rho)H_m^{\prime(1)}(kR)\cos(m(\theta-\phi)), & R>\rho,\\ T^{\mathrm{E}}(s,x)=\frac{-\pi k i}{2}\sum_{m=0}^{\infty}\varepsilon_m H_m^{(1)}(k\rho)J'_m(kR)\cos(m(\theta-\phi)), & \rho>R,\end{cases}\tag{11}$$

$$L(s,x)=\begin{cases} L^{\mathrm{I}}(s,x)=\frac{-\pi k i}{2}\sum_{m=0}^{\infty}\varepsilon_m J'_m(k\rho)H_m^{(1)}(kR)\cos(m(\theta-\phi)), & R>\rho,\\ L^{\mathrm{E}}(s,x)=\frac{-\pi k i}{2}\sum_{m=0}^{\infty}\varepsilon_m H_m^{\prime(1)}(k\rho)J_m(kR)\cos(m(\theta-\phi)), & \rho>R,\end{cases}\tag{12}$$

$$M(s,x)=\begin{cases} M^{\mathrm{I}}(s,x)=\frac{-\pi k^2 i}{2}\sum_{m=0}^{\infty}\varepsilon_m J'_m(k\rho)H_m^{\prime(1)}(kR)\cos(m(\theta-\phi)), & R\geqslant\rho,\\ M^{\mathrm{E}}(s,x)=\frac{-\pi k^2 i}{2}\sum_{m=0}^{\infty}\varepsilon_m H_m^{\prime(1)}(k\rho)J'_m(kR)\cos(m(\theta-\phi)), & \rho>R,\end{cases}\tag{13}$$

where ε_m is the Neumann factor

$$\varepsilon_m=\begin{cases}1, & m=0,\\ 2, & m=1,2,\ldots\infty.\end{cases}\tag{14}$$

Since the potentials resulted from $T(s,x)$ and $L(s,x)$ are discontinuous cross the boundary, the potentials of $T(s,x)$ and $L(s,x)$ for $R\to\rho^+$ and $R\to\rho^-$ are different. This is the reason why $R=\rho$ is not included in the expression for the degenerate kernels of $T(s,x)$ and $L(s,x)$. The analytical evaluation of the integrals for harmonic boundary distribution is listed in the Appendix and they are all nonsingular. The degenerate kernels simply serve as the means to evaluate regular integrals analytically and take the limits analytically. The reason that Eqs. (2) and (8) yield the same algebraic equation when the limit is taken from the inside or from the outside of the region is that both limits represent the algebraic equation that is an approximate counterpart of the boundary integral equation, that for the case of a smooth boundary has in the left-hand side term $\pi u(x)$ or $\pi t(x)$ rather than $2\pi u(x)$ or $2\pi t(x)$ for the domain point or 0 for the point outside the domain. Besides, the limiting case to the boundary is also addressed. The continuous and jump behavior across the boundary is well captured by the Wronskian property of Bessel function J_m and Y_m bases

$$W(J_m(kR),Y_m(kR))=Y'_m(kR)J_m(kR)-Y_m(kR)J'_m(kR)=\frac{2}{\pi kR}\tag{15}$$

as shown below

$$\int_0^{2\pi}(T^{\mathrm{I}}(s,x)-T^{\mathrm{E}}(s,x))\cos(m\theta)R\,\mathrm{d}\theta=2\pi\cos(m\phi),\quad x\in B,\tag{16}$$

$$\int_0^{2\pi}(T^{\mathrm{I}}(s,x)-T^{\mathrm{E}}(s,x))\sin(m\theta)R\,\mathrm{d}\theta=2\pi\sin(m\phi),\quad x\in B,\tag{17}$$

where T^{I} and T^{E} are the interior and exterior expressions for the T kernel in degenerate form. After employing Eqs. (16) and (17), (2) and (8) yields the same linear algebraic equation when x is exactly pushed on the boundary from the domain or the complementing domain. A proof for the Laplace case can be found [18].

In order to fully utilize the geometry of circular boundary, the potential u and its normal flux t can be approximated by employing the Fourier series. Therefore, we obtain

$$u(s)=a_0+\sum_{n=1}^{\infty}(a_n\cos n\theta+b_n\sin n\theta),\quad s\in B,\tag{18}$$

$$t(s)=p_0+\sum_{n=1}^{\infty}(p_n\cos n\theta+q_n\sin n\theta),\quad s\in B,\tag{19}$$

where a_0, a_n, b_n, p_0, p_n and q_n are the Fourier coefficients and θ is the polar angle which is equally discretized. Eqs. (8) and (9) can be easily calculated by employing the orthogonal property of Fourier series. In the real computation, only the finite P terms are used in the summation of Eqs. (18) and (19).

2.4. Adaptive observer system

Since the boundary integral equations are frame indifferent, *i.e.* rule of objectivity is obeyed. Adaptive observer system is chosen to fully employ the property of degenerate kernels. Fig. 2 shows the boundary integration for the circular boundaries. It is worthy noted that the origin of the observer system can be adaptively located on the center of the corresponding circle under integration to fully utilize the geometry of circular boundary. The dummy variable in the integration on the circular boundary is just the angle (θ) instead of the radial coordinate (R). By using the adaptive system, all the boundary integrals can be determined analytically free of principal value.

2.5. Vector decomposition technique for the potential gradient in the hypersingular formulation

Since hypersingular equation plays an important role for dealing with fictitious frequencies, potential gradient of the field quantity is required to calculate. For the eccentric

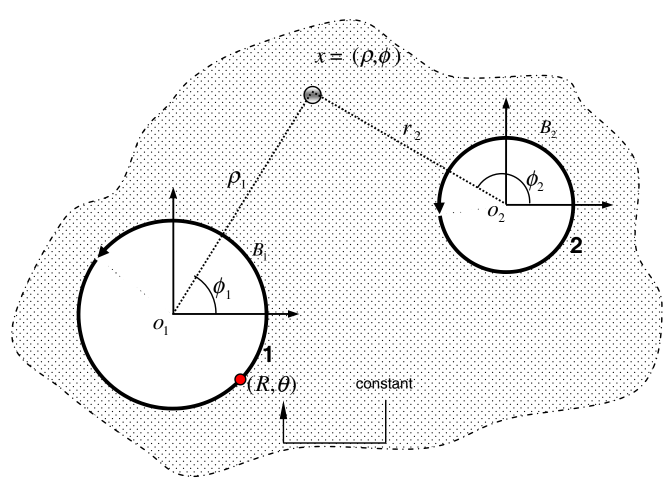

Fig. 2. Adaptive observer system.

case, the field point and source point may not locate on the circular boundaries with the same center except the two points on the same circular boundary or on the annular cases. Special treatment for the normal derivative should be taken care. As shown in Fig. 3 where the origins of observer system are different, the true normal direction $\hat{e}_1$ with respect to the collocation point x on the B_j boundary should be superimposed by using the radial direction $\hat{e}_3$ and angular direction $\hat{e}_4$. We call this treatment "vector decomposition technique". According to the concept, Eqs. (12) and (13) can be modified as

For the B_j integral of the circular boundary, the kernels of $U(s,x), T(s,x) L(s,x)$ and $M(s,x)$ are respectively expressed in terms of degenerate kernels of Eqs. (10), (11), (20) and (21) with respect to the observer origin at the center of B_j. The boundary densities of $u(s)$ and $t(s)$ are substituted by using the Fourier series of Eqs. (18) and (19), respectively. In the B_j integration, we set the origin of the observer system to collocate at the center c_j of B_j to fully utilize the degenerate kernel and Fourier series. By locating the null-field point on the real boundary B_k from outside of the domain D^{E} in numerical implementation, a linear alge-

$$L(s,x) = \begin{cases} L^{\mathrm{I}}(s,x) = \frac{-\pi k i}{2} \sum_{m=-\infty}^{\infty} J'_m(k\rho) H_m^{(1)}(kR)\cos(m(\theta-\phi))\cos(\phi_c-\phi_j), - \frac{m}{k\rho} J_m(k\rho) H_m^{(1)}(kR)\sin(m(\theta-\phi))\sin(\phi_c-\phi_j), & R>\rho, \\ L^{\mathrm{E}}(s,x) = \frac{-\pi k i}{2} \sum_{m=-\infty}^{\infty} H_m'^{(1)}(k\rho) J_m(kR)\cos(m(\theta-\phi))\cos(\phi_c-\phi_j) - \frac{m}{k\rho} J_m(k\rho) H_m^{(1)}(kR)\sin(m(\theta-\phi))\sin(\phi_c-\phi_j), & \rho>R, \end{cases} \tag{20}$$

$$M(s,x) = \begin{cases} M^{\mathrm{I}}(s,x) = \frac{-\pi k i}{2} \sum_{m=-\infty}^{\infty} J'_m(k\rho) H_m'^{(1)}(kR)\cos(m(\theta-\phi))\cos(\phi_c-\phi_j) - \frac{m}{k\rho} J_m(k\rho) H_m'^{(1)}(kR)\sin(m(\theta-\phi))\sin(\phi_c-\phi_j), & R \geqslant \rho, \\ M^{\mathrm{E}}(s,x) = \frac{-\pi k i}{2} \sum_{m=-\infty}^{\infty} H_m'^{(1)}(k\rho) J'_m(kR)\cos(m(\theta-\phi))\cos(\phi_c-\phi_j) - \frac{m}{k\rho} J_m(k\rho) H_m'^{(1)}(kR)\sin(m(\theta-\phi))\sin(\phi_c-\phi_j), & \rho>R. \end{cases} \tag{21}$$

2.6. Linear algebraic equation

In order to calculate the $2P+1$ unknown Fourier coefficients, $2P+1$ boundary points on each circular boundary are needed to be collocated. By collocating the null-field point exactly on the kth circular boundary for Eqs. (8) and (9) as shown in Fig. 4a, we have

$$0 = \sum_{j=1}^{N} \int_{B_j} T(s,x_k) u(s)\, \mathrm{d}B(s) - \sum_{j=1}^{N} \int_{B_j} U(s,x_k) t(s)\, \mathrm{d}B(s), \quad x_k \in D^{\mathrm{E}} \cup B, \tag{22}$$

$$0 = \sum_{j=1}^{N} \int_{B_j} M(s,x_k) u(s)\, \mathrm{d}B(s) - \sum_{j=1}^{N} \int_{B_j} L(s,x_k) t(s)\, \mathrm{d}B(s), \quad x_k \in D^{\mathrm{E}} \cup B, \tag{23}$$

where N is the number of circles. It is noted that the path is anticlockwise for the outer circle. Otherwise, it is clockwise.

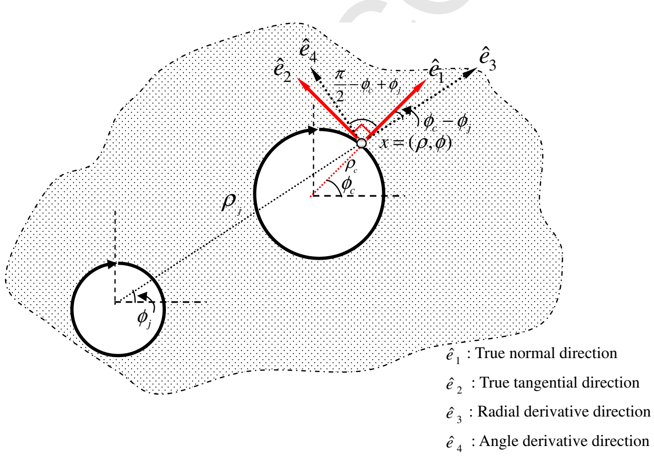

Fig. 3. Vector decomposition for potential gradient in the hypersingular equation.

braic system is obtained

$$[\boldsymbol{U}]\{\boldsymbol{t}\} = [\boldsymbol{T}]\{\boldsymbol{u}\}, \tag{24}$$

$$[\boldsymbol{L}]\{\boldsymbol{t}\} = [\boldsymbol{M}]\{\boldsymbol{u}\}, \tag{25}$$

where $[\boldsymbol{U}], [\boldsymbol{T}], [\boldsymbol{L}]$ and $[\boldsymbol{M}]$ are the influence matrices with a dimension of $N \times (2P+1)$ by $N \times (2P+1)$ and $\{\boldsymbol{t}\}$ and $\{\boldsymbol{u}\}$ denote the vectors for $t(s)$ and $u(s)$ of the Fourier coefficients with a dimension of $N \times (2P+1)$ by 1. where, $[\boldsymbol{U}], [\boldsymbol{T}], [\boldsymbol{L}], [\boldsymbol{M}], \{\boldsymbol{u}\}$ and $\{\boldsymbol{t}\}$ can be defined as follows:

$$[\boldsymbol{U}] = [\boldsymbol{U}_{\alpha\beta}] = \begin{bmatrix} \boldsymbol{U}_{11} & \boldsymbol{U}_{12} & \cdots & \boldsymbol{U}_{1N} \\ \boldsymbol{U}_{21} & \boldsymbol{U}_{22} & \cdots & \boldsymbol{U}_{2N} \\ \vdots & \vdots & \ddots & \vdots \\ \boldsymbol{U}_{N1} & \boldsymbol{U}_{N2} & \cdots & \boldsymbol{U}_{NN} \end{bmatrix}, \quad [\boldsymbol{T}] = [\boldsymbol{T}_{\alpha\beta}] = \begin{bmatrix} \boldsymbol{T}_{11} & \boldsymbol{T}_{12} & \cdots & \boldsymbol{T}_{1N} \\ \boldsymbol{T}_{21} & \boldsymbol{T}_{22} & \cdots & \boldsymbol{T}_{2N} \\ \vdots & \vdots & \ddots & \vdots \\ \boldsymbol{T}_{N1} & \boldsymbol{T}_{N2} & \cdots & \boldsymbol{T}_{NN} \end{bmatrix}, \tag{26}$$

$$[\boldsymbol{L}] = [\boldsymbol{L}_{\alpha\beta}] = \begin{bmatrix} \boldsymbol{L}_{11} & \boldsymbol{L}_{12} & \cdots & \boldsymbol{L}_{1N} \\ \boldsymbol{L}_{21} & \boldsymbol{L}_{22} & \cdots & \boldsymbol{L}_{2N} \\ \vdots & \vdots & \ddots & \vdots \\ \boldsymbol{L}_{N1} & \boldsymbol{L}_{N2} & \cdots & \boldsymbol{L}_{NN} \end{bmatrix}, \quad [\boldsymbol{M}] = [\boldsymbol{M}_{\alpha\beta}] = \begin{bmatrix} \boldsymbol{M}_{11} & \boldsymbol{M}_{12} & \cdots & \boldsymbol{M}_{1N} \\ \boldsymbol{M}_{21} & \boldsymbol{M}_{22} & \cdots & \boldsymbol{M}_{2N} \\ \vdots & \vdots & \ddots & \vdots \\ \boldsymbol{M}_{N1} & \boldsymbol{M}_{N2} & \cdots & \boldsymbol{M}_{NN} \end{bmatrix}, \tag{27}$$

$$\{\boldsymbol{u}\} = \begin{Bmatrix} \boldsymbol{u}_1 \\ \boldsymbol{u}_2 \\ \boldsymbol{u}_3 \\ \vdots \\ \boldsymbol{u}_N \end{Bmatrix}, \quad \{\boldsymbol{t}\} = \begin{Bmatrix} \boldsymbol{t}_1 \\ \boldsymbol{t}_2 \\ \boldsymbol{t}_3 \\ \vdots \\ \boldsymbol{t}_N \end{Bmatrix}, \tag{28}$$

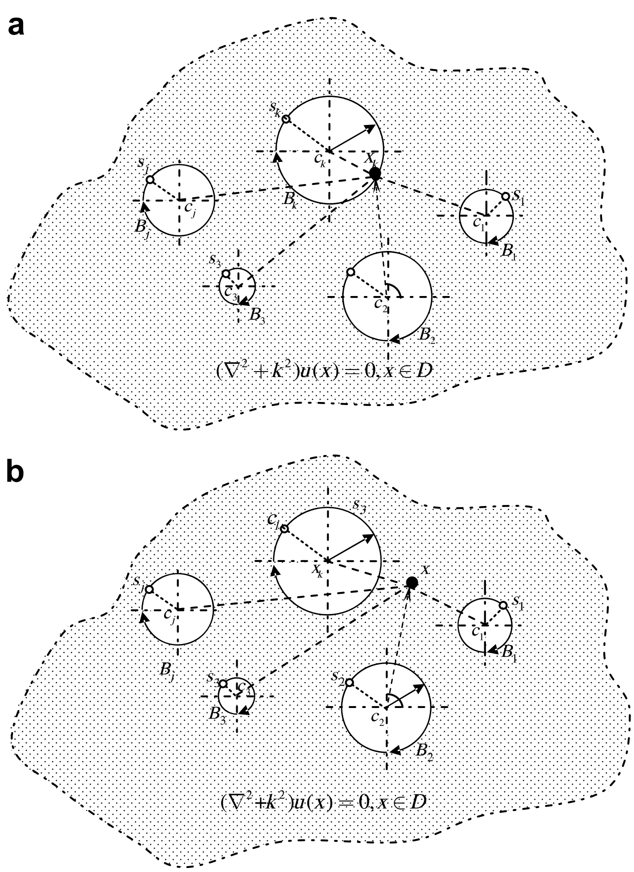

Fig. 4. Boundary integral formulation: (a) null-field integral equation (x move to B from D^{E}) and (b) boundary integral equation for the domain point.

where the vectors $\{\boldsymbol{u}_k\}$ and $\{\boldsymbol{t}_k\}$ are in the form of $\{a_0^k \quad a_1^k \quad b_1^k \quad \cdots \quad a_P^k \quad b_P^k\}^{\mathrm{T}}$ and $\{p_0^k \quad p_1^k \quad q_1^k \quad \cdots \quad p_P^k q_P^k\}^{\mathrm{T}}$; the first subscript "$\alpha$" ($\alpha = 1, 2, \ldots, N$) in the $[\boldsymbol{U}_{\alpha\beta}]$ denotes the index of the αth circle where the collocation point is located and the second subscript "β" ($\beta = 1, 2 \ldots, N$) denotes the index of the βth circle where the boundary data $\{\boldsymbol{u}_k\}$ or $\{\boldsymbol{t}_k\}$ are specified. N is the number of circular holes in the domain and P indicates the highest harmonic of truncated terms in Fourier series. The coefficient matrix of the linear algebraic system is partitioned into blocks, and each diagonal block (U_{pp}, p no sum) corresponds to the influence matrices due to the same circle of collocation and Fourier expansion. After uniformly collocating the point along the αth circular boundary, the sub-matrix can be written as

$$[U_{\alpha\beta}] = \begin{bmatrix} U_{\alpha\beta}^{0c}(\phi_1) & U_{\alpha\beta}^{1c}(\phi_1) & U_{\alpha\beta}^{1s}(\phi_1) & \cdots & U_{\alpha\beta}^{Pc}(\phi_1) & U_{\alpha\beta}^{Ps}(\phi_1) \\ U_{\alpha\beta}^{0c}(\phi_2) & U_{\alpha\beta}^{1c}(\phi_2) & U_{\alpha\beta}^{1s}(\phi_2) & \cdots & U_{\alpha\beta}^{Pc}(\phi_2) & U_{\alpha\beta}^{Ps}(\phi_2) \\ U_{\alpha\beta}^{0c}(\phi_3) & U_{\alpha\beta}^{1c}(\phi_3) & U_{\alpha\beta}^{1s}(\phi_3) & \cdots & U_{\alpha\beta}^{Pc}(\phi_3) & U_{\alpha\beta}^{Ps}(\phi_3) \\ \vdots & \vdots & \vdots & \ddots & \vdots & \vdots \\ U_{\alpha\beta}^{0c}(\phi_{2P}) & U_{\alpha\beta}^{1c}(\phi_{2P}) & U_{\alpha\beta}^{1s}(\phi_{2P}) & \cdots & U_{\alpha\beta}^{Mc}(\phi_{2P}) & U_{\alpha\beta}^{Ms}(\phi_{2P}) \\ U_{\alpha\beta}^{0c}(\phi_{2P+1}) & U_{\alpha\beta}^{1c}(\phi_{2P+1}) & U_{\alpha\beta}^{1s}(\phi_{2P+1}) & \cdots & U_{\alpha\beta}^{Mc}(\phi_{2P+1}) & U_{\alpha\beta}^{Ms}(\phi_{2P+1}) \end{bmatrix}, \tag{29}$$

$$[T_{\alpha\beta}] = \begin{bmatrix} T_{\alpha\beta}^{0c}(\phi_1) & T_{\alpha\beta}^{1c}(\phi_1) & T_{\alpha\beta}^{1s}(\phi_1) & \cdots & T_{\alpha\beta}^{Pc}(\phi_1) & T_{\alpha\beta}^{Ps}(\phi_1) \\ T_{\alpha\beta}^{0c}(\phi_2) & T_{\alpha\beta}^{1c}(\phi_2) & T_{\alpha\beta}^{1s}(\phi_2) & \cdots & T_{\alpha\beta}^{Pc}(\phi_2) & T_{\alpha\beta}^{Ps}(\phi_2) \\ T_{\alpha\beta}^{0c}(\phi_3) & T_{\alpha\beta}^{1c}(\phi_3) & T_{\alpha\beta}^{1s}(\phi_3) & \cdots & T_{\alpha\beta}^{Pc}(\phi_3) & T_{\alpha\beta}^{Ps}(\phi_3) \\ \vdots & \vdots & \vdots & \ddots & \vdots & \vdots \\ T_{\alpha\beta}^{0c}(\phi_{2P}) & T_{\alpha\beta}^{1c}(\phi_{2P}) & T_{\alpha\beta}^{1s}(\phi_{2P}) & \cdots & T_{\alpha\beta}^{Pc}(\phi_{2P}) & T_{\alpha\beta}^{Ps}(\phi_{2P}) \\ T_{\alpha\beta}^{0c}(\phi_{2P+1}) & T_{\alpha\beta}^{1c}(\phi_{2P+1}) & T_{\alpha\beta}^{1s}(\phi_{2P+1}) & \cdots & T_{\alpha\beta}^{Pc}(\phi_{2P+1}) & T_{\alpha\beta}^{Ps}(\phi_{2P+1}) \end{bmatrix}, \tag{30}$$

$$[L_{\alpha\beta}] = \begin{bmatrix} L_{\alpha\beta}^{0c}(\phi_1) & L_{\alpha\beta}^{1c}(\phi_1) & L_{\alpha\beta}^{1s}(\phi_1) & \cdots & L_{\alpha\beta}^{Pc}(\phi_1) & L_{\alpha\beta}^{Ps}(\phi_1) \\ L_{\alpha\beta}^{0c}(\phi_2) & L_{\alpha\beta}^{1c}(\phi_2) & L_{\alpha\beta}^{1s}(\phi_2) & \cdots & L_{\alpha\beta}^{Pc}(\phi_2) & L_{\alpha\beta}^{Ps}(\phi_2) \\ L_{\alpha\beta}^{0c}(\phi_3) & L_{\alpha\beta}^{1c}(\phi_3) & L_{\alpha\beta}^{1s}(\phi_3) & \cdots & L_{\alpha\beta}^{Pc}(\phi_3) & L_{\alpha\beta}^{Ps}(\phi_3) \\ \vdots & \vdots & \vdots & \ddots & \vdots & \vdots \\ L_{\alpha\beta}^{0c}(\phi_{2P}) & L_{\alpha\beta}^{1c}(\phi_{2P}) & L_{\alpha\beta}^{1s}(\phi_{2P}) & \cdots & L_{\alpha\beta}^{Pc}(\phi_{2P}) & L_{\alpha\beta}^{Ps}(\phi_{2P}) \\ L_{\alpha\beta}^{0c}(\phi_{2P+1}) & L_{\alpha\beta}^{1c}(\phi_{2P+1}) & L_{\alpha\beta}^{1s}(\phi_{2P+1}) & \cdots & L_{\alpha\beta}^{Pc}(\phi_{2P+1}) & L_{\alpha\beta}^{Ps}(\phi_{2P+1}) \end{bmatrix}, \tag{31}$$

$$[M_{\alpha\beta}] = \begin{bmatrix} M_{\alpha\beta}^{0c}(\phi_1) & M_{\alpha\beta}^{1c}(\phi_1) & M_{\alpha\beta}^{1s}(\phi_1) & \cdots & M_{\alpha\beta}^{Pc}(\phi_1) & M_{\alpha\beta}^{Ps}(\phi_1) \\ M_{\alpha\beta}^{0c}(\phi_2) & M_{\alpha\beta}^{1c}(\phi_2) & M_{\alpha\beta}^{1s}(\phi_2) & \cdots & M_{\alpha\beta}^{Pc}(\phi_2) & M_{\alpha\beta}^{Ps}(\phi_2) \\ M_{\alpha\beta}^{0c}(\phi_3) & M_{\alpha\beta}^{1c}(\phi_3) & M_{\alpha\beta}^{1s}(\phi_3) & \cdots & M_{\alpha\beta}^{Pc}(\phi_3) & M_{\alpha\beta}^{Ps}(\phi_3) \\ \vdots & \vdots & \vdots & \ddots & \vdots & \vdots \\ M_{\alpha\beta}^{0c}(\phi_{2P}) & M_{\alpha\beta}^{1c}(\phi_{2P}) & M_{\alpha\beta}^{1s}(\phi_{2P}) & \cdots & M_{\alpha\beta}^{Pc}(\phi_{2P}) & M_{\alpha\beta}^{Ps}(\phi_{2P}) \\ M_{\alpha\beta}^{0c}(\phi_{2P+1}) & M_{\alpha\beta}^{1c}(\phi_{2P+1}) & M_{\alpha\beta}^{1s}(\phi_{2P+1}) & \cdots & M_{\alpha\beta}^{Pc}(\phi_{2P+1}) & M_{\alpha\beta}^{Ps}(\phi_{2P+1}) \end{bmatrix}. \tag{32}$$

It is noted that the superscript "0s" in Eq. (29) disappears since $\sin(0\theta) = 0$. And the element of $[U_{\alpha\beta}], [T_{\alpha\beta}], [L_{\alpha\beta}]$ and $[M_{\alpha\beta}]$ are defined as

$$U_{\alpha\beta}^{nc} = \int_{B_k} U(s_k, x_m)\cos(n\theta_k)R_k\,\mathrm{d}\theta_k, \quad n = 0, 1, 2\ldots, P, \tag{33}$$

$$U_{\alpha\beta}^{ns} = \int_{B_k} U(s_k, x_m)\sin(n\theta_k)R_k\,\mathrm{d}\theta_k, \quad n = 0, 1, 2\ldots, P, \tag{34}$$

$$T_{\alpha\beta}^{nc} = \int_{B_k} T(s_k, x_m)\cos(n\theta_k)R_k\,\mathrm{d}\theta_k, \quad n = 0, 1, 2\ldots, P, \tag{35}$$

$$T_{\alpha\beta}^{ns} = \int_{B_k} T(s_k, x_m)\sin(n\theta_k)R_k\,\mathrm{d}\theta_k, \quad n = 0, 1, 2\ldots, P, \tag{36}$$

$$L_{\alpha\beta}^{nc} = \int_{B_k} L(s_k, x_m)\cos(n\theta_k)R_k\,\mathrm{d}\theta_k, \quad n = 0, 1, 2\ldots, P, \tag{37}$$

$$L_{\alpha\beta}^{ns} = \int_{B_k} L(s_k, x_m)\sin(n\theta_k)R_k\,\mathrm{d}\theta_k, \quad n = 0, 1, 2\ldots, P, \tag{38}$$

$$M_{\alpha\beta}^{nc} = \int_{B_k} L(s_k, x_m)\cos(n\theta_k)R_k\,\mathrm{d}\theta_k, \quad n = 0, 1, 2\ldots, P, \tag{39}$$

$$M_{\alpha\beta}^{nc} = \int_{B_k} L(s_k, x_m)\cos(n\theta_k)R_k\,\mathrm{d}\theta_k, \quad n = 0, 1, 2\ldots, P, \tag{40}$$

where $\phi_m, m = 1, 2\ldots, 2P+1$ is the polar angle of the collocating points x_m around boundary. After obtaining the

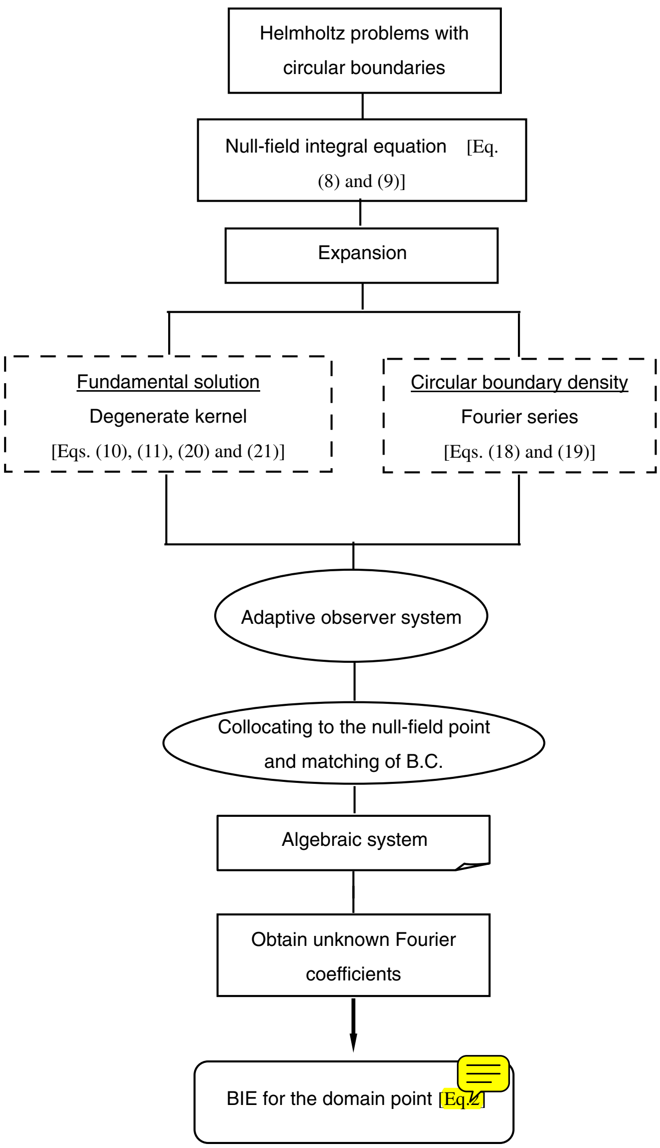

Fig. 5. The flowchart of the present method.

unknown Fourier coefficients, the origin of observer system is set to c_j in the B_j integration as shown in Fig. 4b to obtain the interior potential by employing Eq. (2). The flowchart of the present method is shown in Fig. 5 and the difference with BEM is shown in Table 1.

3. Numerical results and discussion

Example 1. Nonuniform radiation problem for one radiator (Neumann boundary condition).

A non-uniform radiation problem from a sector of a cylinder is considered (Neumann boundary) as shown in Fig. 6. The analytical solution is [19]

$$u(r,\theta) = -\frac{2}{\pi k}\sum_{n=0}^{\infty}{}' \frac{\sin n\alpha}{n}\frac{H_n^{(1)}(kr)}{H_n'^{(1)}(ka)}\cos n\theta,$$
$$r \geqslant a, \quad 0 \leqslant \theta \leqslant 2\pi. \tag{41}$$

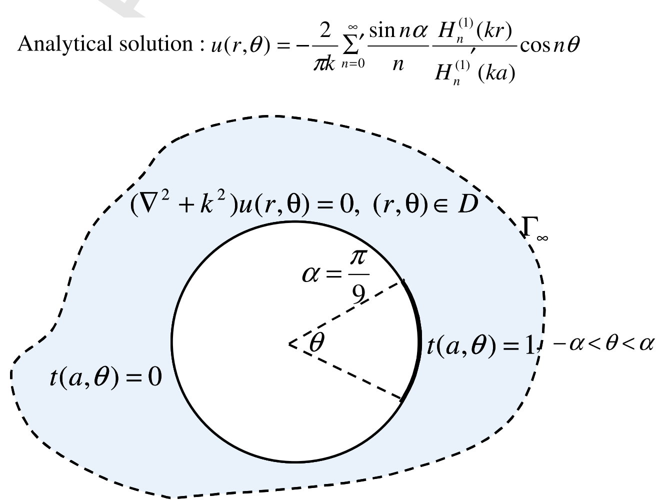

Fig. 6. Nonuniform radiator problem (Neumann).

Table 1
The difference between the present method and BEM

Method	System				
	Boundary density discretization	Auxiliary system	Coordinate system	Boundary integral	Formulation
Present method	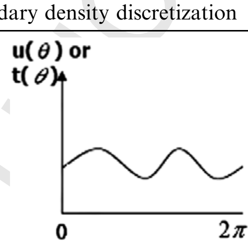	Degenerate kernel	Adaptive observer system	No principal value	Null-field integral equations
BEM	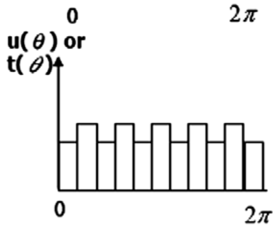	Fundamental solution	Fixed observer system	Principal values (CPV, RPV and HPV)	Boundary integral equation for boundary point

where RPV, CPV and HPV denote Riemann principal value, Cauchy principal value and Hadamard principal value.

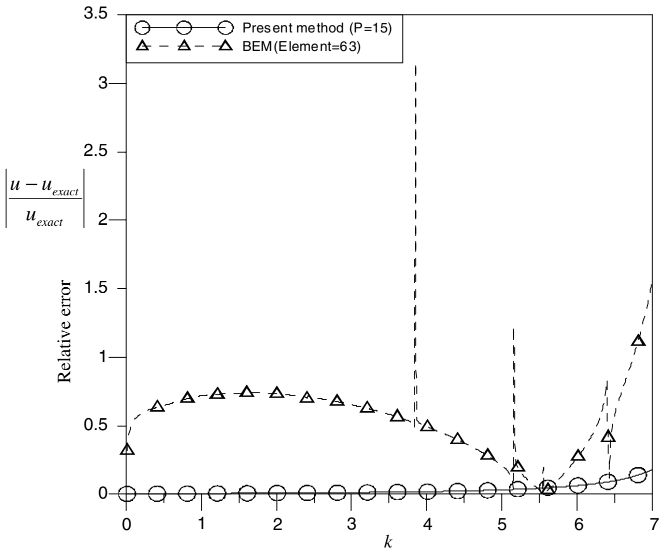

Fig. 7. The error analysis between the present method and BEM.

We select $\alpha = \pi/9$ and $ka = 1.0$. Fig. 7 shows the error analysis for the present method and BEM after comparing with the analytical solution. It can be found that the present method is superior to BEM. The analytical solution is obtained by using 15 terms in the series representations. By adopting the truncated Fourier series ($P = 15$) in our formulation, the contour plot is obtained. Sixty-three constant elements are adopted in the dual BEM [3]. It is found that we can obtain the acceptable results by using fewer numbers of degrees of freedom in comparison with BEM results. The comparison seems unfair for the problems with circular boundaries. But the main gains of the present method are the exponential convergence and free of boundary layer effect where two references [20,21] can support this point.

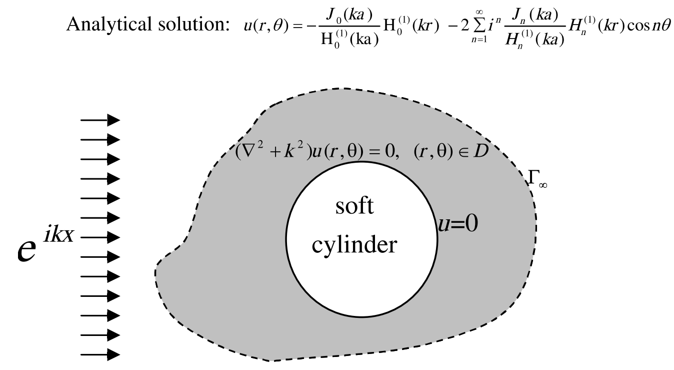

Fig. 9. Sketch of the scattering problem (Dirichlet condition) for a cylinder.

Example 2. Scattering problem for one scatter (Dirichlet boundary condition).

For the scattering problem subject to the incident wave, this problem can be decomposed into two parts, (a) incident wave field and (b) radiation field, as shown in

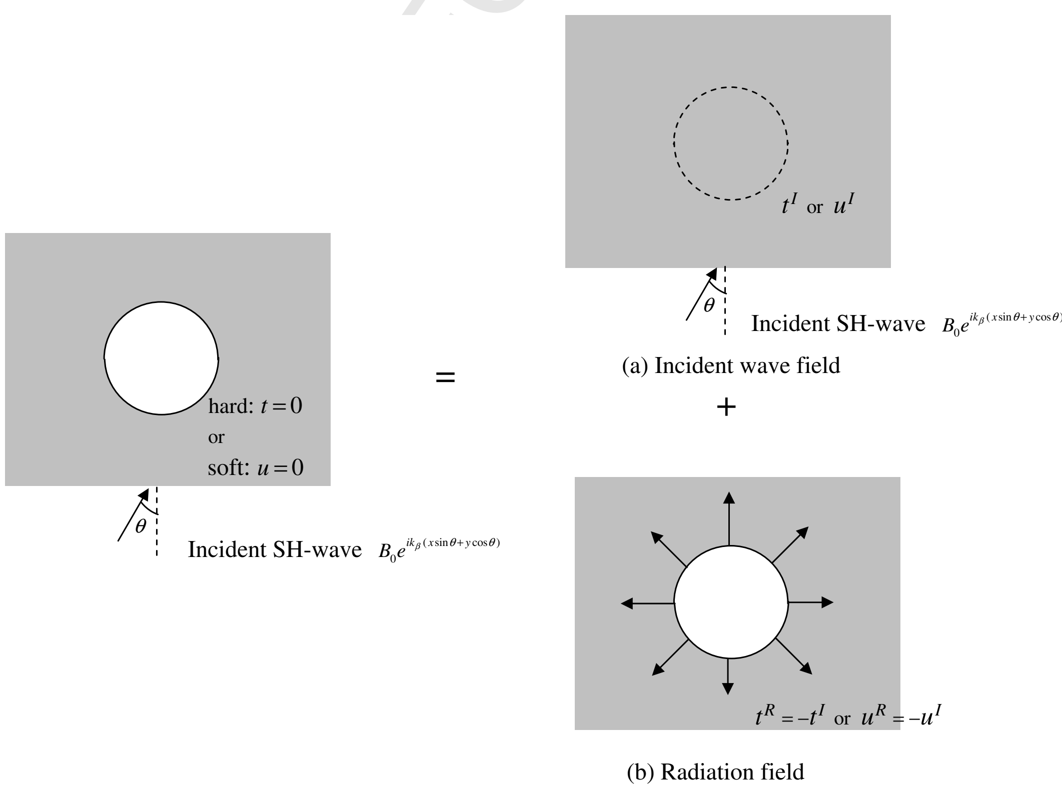

Fig. 8. The decomposition of superposition of scattering problem into (a) incident wave field and (b) radiation field.

Please cite this article in press as: J.T. Chen et al., A semi-analytical approach for radiation and scattering ..., Comput. Methods Appl. Mech. Eng. (2007), doi:10.1016/j.cma.2007.02.004

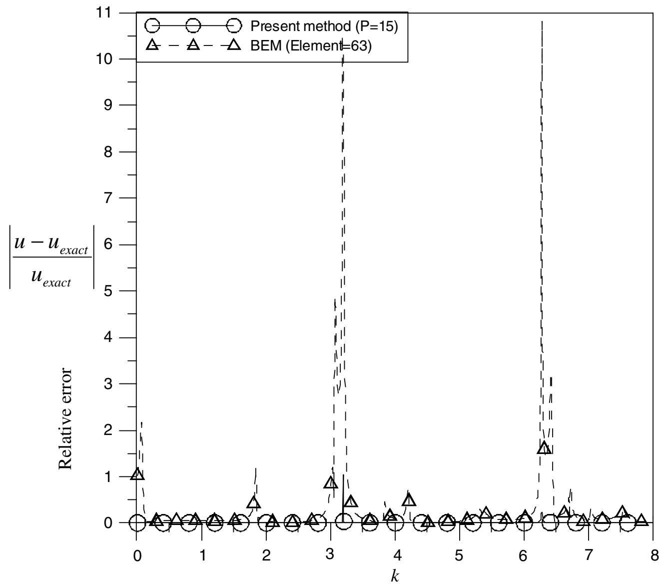

Fig. 10. The error analysis between present method and BEM.

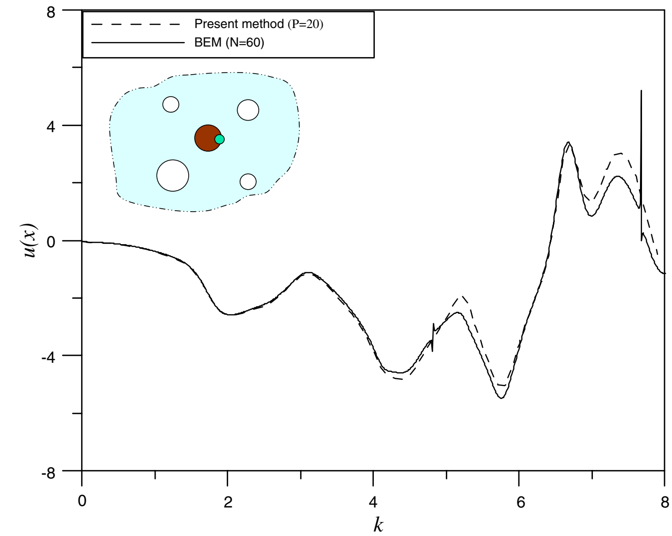

Fig. 12. The positions of irregular values using different methods of center circle.

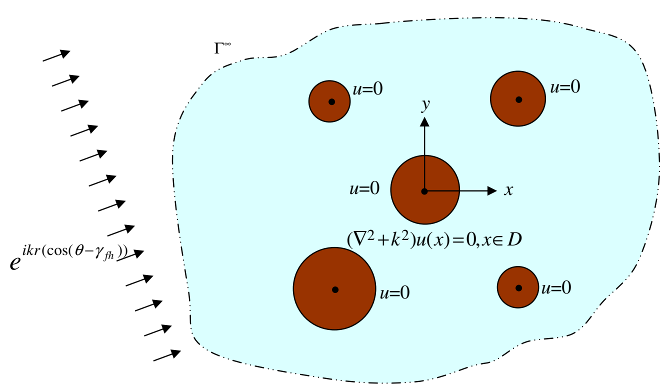

Fig. 11. The plane wave scattering by five circular cylinders with the center positions ((0, 0), (1.5, 1.5), (−1.5, 1.5), (−1.5, −1.5), (1.5, −1.5)) and the corresponding radii (0.5, 0.4, 0.3, 0.6, 0.3), (1) $k=\pi$ and (2) $k=8\pi$, incidence angle $\gamma_{fh}=\frac{\pi}{8}$.

Fig. 8. By matching the boundary condition, the radiation boundary condition in part (b) is obtained as the minus quantity of incident wave function, e.g. $t^{\mathrm{Ra}}=-t^{\mathrm{In}}$ for hard scatter or $u^{\mathrm{Ra}}=-u^{\mathrm{In}}$ for soft scatter, respectively where the superscripts Ra and In mean radiation and incidence, respectively.

Plane wave scattering for a soft circular cylinder (Dirichlet boundary condition) is considered in Fig. 9. The analytical solution is

$$u(r,\theta)=-\frac{J_0(ka)}{H_0^{(1)}(ka)}H_0^{(1)}(kr)-2\sum_{n=1}^{\infty}i^n\frac{J_n(ka)}{H_n^{(1)}(ka)}H_n^{(1)}(kr)\cos n\theta,$$
$$r\geqslant a,\quad 0\leqslant\theta\leqslant 2\pi. \tag{42}$$

Fig. 10 shows the error analysis for the present method and BEM. It can be found that the present result is superior to that of BEM. Large errors in the irregular case by using BEM are found. The analytical solution is obtained by using fifteen terms in the series representations. By adopting the truncated Fourier series ($P=15$) in our formulation, the contour plot is obtained. Sixty-three constant elements are adopted in the dual BEM. Similarly, less degree of freedom is required in our formulation (31 points) to have the good accuracy after comparing with the data of BEM (63 elements) [3].

Example 3. Scattering problem for five scatters (Dirichlet boundary condition).

To demonstrate the generality of our approach for arbitrary number of radiators and scatters, plane wave scattering by five soft circular cylinders (Dirichlet boundary condition) is considered in Fig. 11. This problem was solved by using the multiple DtN approach [13]. In Fig. 12, irregular frequencies do not appear by using the present method but osculation of irregular frequencies occur by using BEM. Numerical instability of zero divided by zero in case of irregular values is overcome due to the semi-analytical nature of the present method [3,4]. For the purpose of comparisons, we choose the data on the artificial boundary versus θ with respect to each cylinder as show in Figs. 13 and 14. Good agreement is made. Regarding to calculation of the higher-order Hankel function, it may need special treatment. In this case, the maximum order is twenty. The computation using IMSL package for the higher-order Hankel function is feasible.

4. Conclusions

For the radiation and scattering problems with circular boundaries, we have proposed a BIEM formulation by

Please cite this article in press as: J.T. Chen et al., A semi-analytical approach for radiation and scattering ..., Comput. Methods Appl. Mech. Eng. (2007), doi:10.1016/j.cma.2007.02.004

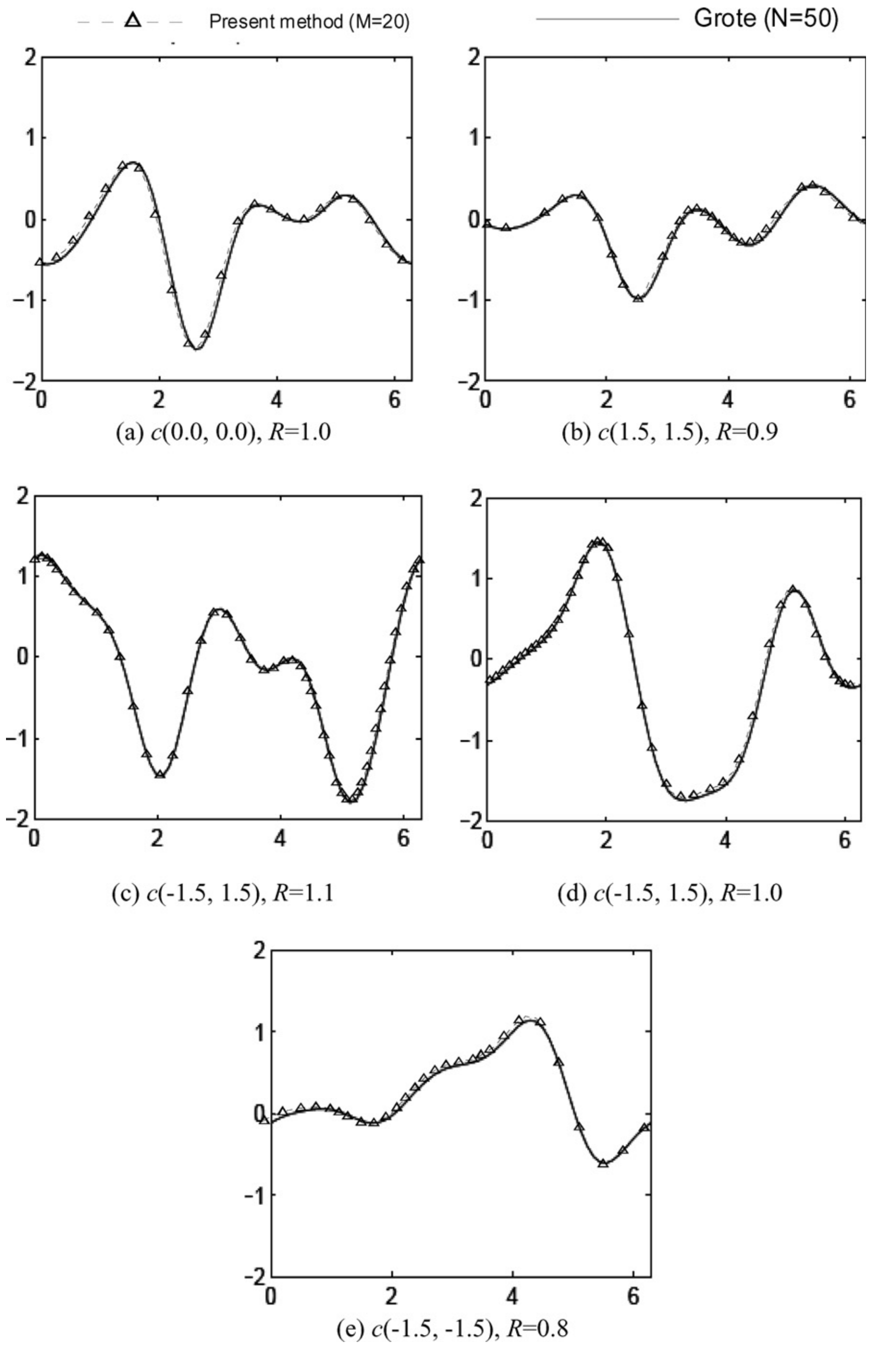

Fig. 13. The real part of total field for the data for the five artificial boundaries versus θ by using different methods for $k = \pi$.

using degenerate kernels, null-field integral equation and Fourier series in companion with adaptive observer systems and vector decomposition. This method is a semi-analytical approach for problems with circular boundaries since only truncation error in the Fourier series is involved. The method shows great generality and versatility for the problems with multiple scatters or radiators of arbitrary radii and positions. Neither hypersingular formulation of Burton and Miller approach nor CHIEF method are required to overcome the fictitious frequencies. An acoustic problem of five scatters in the infinite plane was solved and the results were compared well with those of Grote and Kirsch.

Acknowledgement

Financial support from the National Science Council under Grant No. NSC 94-2115-M-019-003 for National Taiwan Ocean University is gratefully acknowledged.

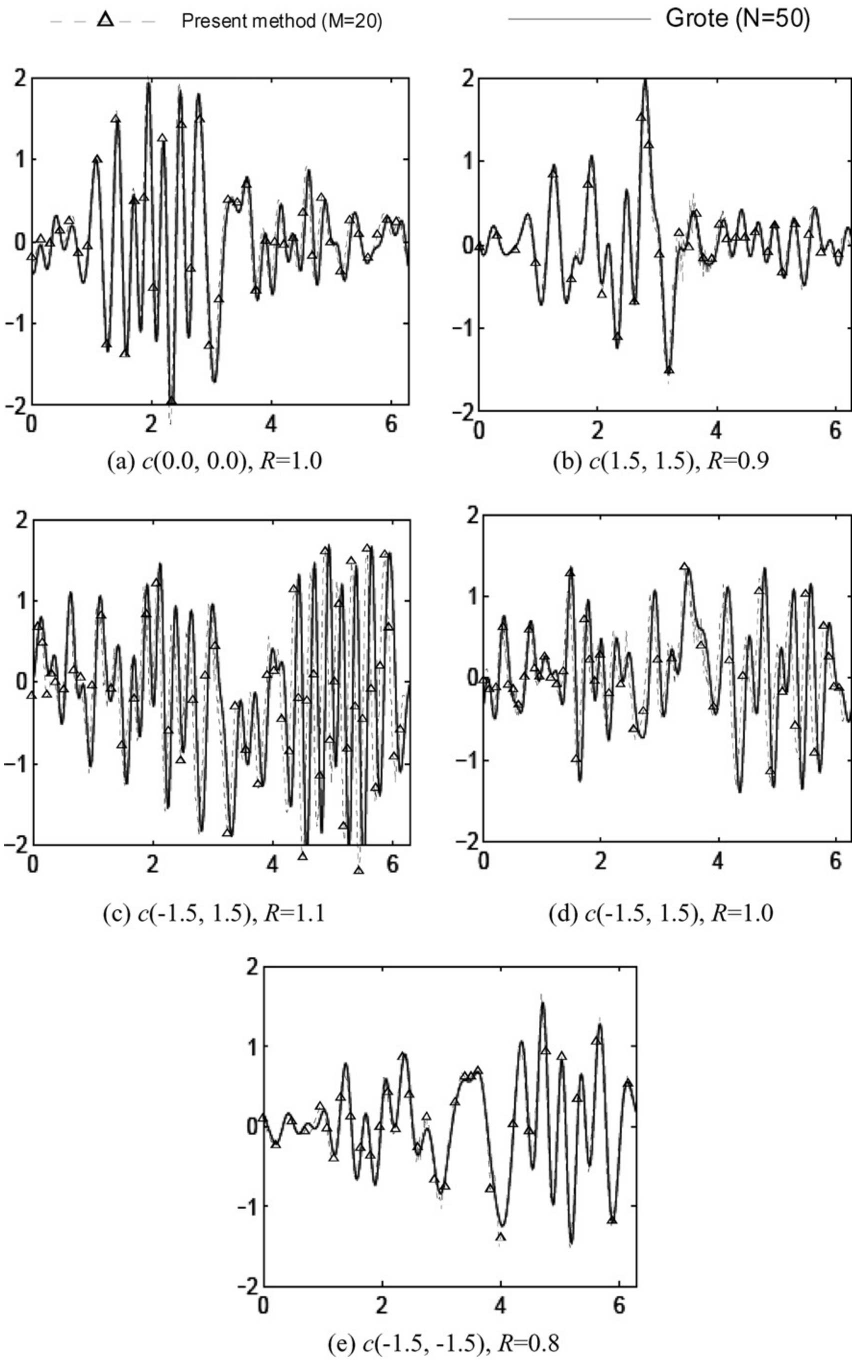

Fig. 14. The real part of total field for the data on the five artificial boundaries versus θ by using different methods for $k = 8\pi$.

Appendix 1

Analytical evaluation of the integrals for the kernels ($T(s,x)$ and $L(s,x)$) and their limit across the boundary.

References

[1] A.J. Burton, G.F. Miller, The application of integral equation methods to numerical solution of some exterior boundary value problems, Proc. Roy. Soc. Lon. Ser. A 323 (1971) 201–210.

[2] H.A. Schenck, Improved integral formulation for acoustic radiation problem, J. Acoust. Soc. Am. 44 (1968) 41–58.

[3] J.T. Chen, K.H. Chen, I.L. Chen, L.W. Liu, A new concept of modal participation factor for numerical instability in the dual BEM for exte- rior acoustics, Mech. Res. Comm. 26 (2) (2003) 161–174.

[4] J.T. Chen, I.L. Chen, K.H. Chen, A unified formulation for the spurious and fictitious frequencies in acoustics using the singular value decomposition and Fredholm alternative theorem, J. Comp. Acoust. 14 (2) (2006) 157–183.

[5] A.F. Seybert, T.K. Rengarajan, The use of CHIEF to obtain unique solutions for acoustic radiation using boundary integral equations, J. Acoust. Soc. Am. 81 (1968) 1299–1306.

[6] T.W. Wu, A.F. Seybert, A weighted residual formulation for the CHIEF method in acoustics, J. Acoust. Soc. Am. 90 (3) (1991) 1608–1614.

Please cite this article in press as: J.T. Chen et al., A semi-analytical approach for radiation and scattering ..., Comput. Methods Appl. Mech. Eng. (2007), doi:10.1016/j.cma.2007.02.004

[7] L. Lee, T.W. Wu, An enhanced CHIEF method for steady-state elastodynamics, Engrg. Anal. Bound. Elem. 12 (1993) 75–83.
[8] S. Ohmatsu, A new simple method to eliminate the irregular frequencies in the theory of water wave radiation problems, Papers of Ship Research Institute 70 (1983).
[9] I.L. Chen, Using the method of fundamental solutions in conjunction with the degenerate kernel in cylindrical acoustic problems, J. Chinese Inst. Engrg. 29 (3) (2006) 445–457.
[10] E. Dokumaci, A.S. Sarigül, Analysis of the near field acoustic radiation characteristics of two radially vibrating spheres by the Helmholtz integral equation formulation and a critical study of the efficacy of the CHIEF over determination method in two-body problems, J. Sound Vib. 187 (5) (1995) 781–798.
[11] C.M. Linton, D.V. Evans, The interaction of waves with arrays of vertical circular cylinders, J. Fluid Mech. 215 (1990) 549–569.
[12] M. Kitahara, Boundary integral equation methods in eigenval problems of elastodynamics and thin plates, Elesvier, Amsterdam.
[13] A.Z. Elsherbeni, M. Hamid, Scattering by parallel conducting circular cylinders, IEEE Trans. Antennas. Propag. 35 (1987) 355–358.
[14] M.J. Grote, C. Kirsch, Dirichlet to Neumann boundary conditions for multiple scattering problems, J. Comp. Phys. 201 (2004) 630–650.
[15] R. Kress, Linear Integral Equations, Springer-verlag, Berlin, 1989.
[16] R. Kress, On the numerical solution of a hypersingular integral equation in scattering theory, J. Comput. Appl. Math. 61 (1995) 345–360.
[17] L.C. Wrobel, The boundary element method, Applications in Thermo-Fluids and Acoustics, vol. 1, Wiley, 2002.
[18] J.T. Chen, W.C. Shen, A.C. Wu, Null-field integral equations for stress field around circular holes under antiplane shear, Engrg. Anal. Bound. Elem. 30 (2006) 205–217.
[19] I. Harari, P.E. Barbone, M. Slavutin, R. Shalom, ‘‘Boundary infinite elements for the Helmholtz equation in exterior domains, Int. J. Numer. Meth. Engrg. 41 (1998) 1105–1131.
[20] J.T. Chen, A.C. Wu, Null-field integral equation approach for multi-inclusion problem under anti-plane shear, ASME, J. Appl. Mech., May, in press.
[21] J.T. Chen, C.C. Hsiao, S.Y. Leu, Null-field integral equation approach for plate problems with circular holes, ASME, J. Appl. Mech. 73 (4) (2006) 679–693.

Please cite this article in press as: J.T. Chen et al., A semi-analytical approach for radiation and scattering ..., Comput. Methods Appl. Mech. Eng. (2007), doi:10.1016/j.cma.2007.02.004